Floating Zone Growth of $Bi_2Sr_2Ca_2Cu_3O_y$ Superconductor

Andrey Maljuk [1,*] and C. T. Lin [2]

[1] Leibniz Institute for Solid State and Materials Research Dresden, D-01171 Dresden, Germany

[2] Max Planck Institute for Solid State Research, D-70569 Stuttgart, Germany, ct.lin@fkf.mpg.de

[*] Correspondence: a.malyuk@ifw-dresden.de; Tel.: +49-351-4659-633

Abstract: The crystal growth of high-temperature oxide superconductors has been hampered by the complexities of these materials and the lack of knowledge of corresponding phase diagrams. The most common crystal growth technique adopted for these materials is the so-called "Flux" method. This method, however, suffers from several drawbacks: (i) crystals are often crucible and flux contaminated; (ii) crystals are difficult to detach from solidified melt; and (iii) crystals are rather small. In most cases, these drawbacks can be overcome by the crucible-free floating zone method. Moreover, this technique is suitable for crystal growth of incongruently melting compounds, and has been thus successfully used to make large single crystals of $Bi_2Sr_2Ca_2Cu_3O_y$ superconductor. In this review, the authors summarize the published and their own growth efforts as well as detailed characterization of as-grown and post-growth annealed samples. The optimal growth conditions that allowed one to obtain the large-size, almost single phase and homogeneous in composition $Bi_2Sr_2Ca_2Cu_3O_y$ single crystals are presented. The effect of long lasting post-growth heat treatment on both crystal quality and superconducting properties has also been demonstrated.

1. Introduction

Since the discovery of high-temperature (high-T_c) superconductivity (SC) in cuprates by Nobel Prize winners J.G. Bednorz and K.A. Müller in 1986, a tremendous work has been done in synthesis of these materials. Here, a crystal growth of high-T_c superconductors plays an extremely important role for the fundamental research because physicists strongly need large size and high quality single crystals to study anisotropic physical properties of these materials. For the Bi-based superconductors, a homologous family with a general formula $Bi_2Sr_2Ca_{n-1}Cu_nO_y$ where $n = 1$, 2 and 3 is known, and superconducting temperature, T_c, strongly varies with the number of CuO_2 layers, n: $T_c \sim 10$ K ($n = 1$), $T_c \approx 80$–90 K ($n = 2$) and $T_c \sim 110$ K ($n = 3$). It is worth mentioning that real materials are always nonstoichiometric with respect to both metallic and oxygen elements. The atomic positions in real crystals structures are also well shifted from the "ideal" ones that lead to incommensurate, quasi one-dimensional structural modulations in all Bi-based compounds. All together, it makes the superconducting properties of single crystals highly sensitive to the history of samples preparation. From this point, a detailed and accurate characterization of as-grown samples becomes very important. In addition, our knowledge of the corresponding quaternary Bi_2O_3-SrO-CaO-CuO phase diagram is quite insufficient [1], which complicates the growth of high quality superconducting single crystals in this system even more.

The quasi two-dimensional crystal structures of all Bi-based oxides also make the growth rate highly anisotropic and this tendency dramatically increased from $n = 1$ to $n = 3$. Therefore, even

nowadays, it is very hard to prepare bulk and single-phase crystals of $Bi_2Sr_2Ca_2Cu_3O_y$ material. Both $Bi_2Sr_2Cu_1O_y$ [2] (hereafter Bi-2201) and $Bi_2Sr_2Ca_1Cu_2O_y$ [3] (hereafter Bi-2212) superconductors have been available as sizeable high-quality single crystals and extensively studied so far [4,5]. On the other hand, fundamental investigations on the three-layered $Bi_2Sr_2Ca_2Cu_3O_y$ compound (hereafter Bi-2223) have been strongly embarrassed due to the lack of high quality single crystals. Even more, the Pb-doped Bi-2223 compound is nowadays believed to be the most promising material for large-scale applications of high-T_c superconductivity at liquid nitrogen temperature, and has been the subject of tremendous studies in the past 20 years. However, all these studies were done on powder/ceramic samples with small grain sizes and can be questioned because of significant boundary effects on sample properties. For example, the pinning characteristics of the Bi-2223 material in the absence of grain boundaries have still been largely unexplored due to the lack of high quality single crystalline samples. It is worth mentioning that pinning properties play the key role in all possible commercial applications of Bi-2223 material.

Figure 1 is a model for the fundamental unit cell of the Bi-2223 phase. The structure has a pseudotetragonal symmetry with lattice parameters $a \sim b$ = 5.4 Å and c = 37.0 Å. The values change slightly depending on the cation, either substitution or non-stoichiometry, which occurs widely in this phase. The Bi-2223 structure contains three CuO_2 sheets in a single CuO_2 block, which are separated by layers of Ca ions. In the central CuO_2 sheet, each copper atom is surrounded by four oxygen atoms. The copper atoms in the outer CuO_2 sheets are in the center of the basal plane of an oxygen pyramid. Adjacent CuO_2 blocks are separated by SrO-BiO-BiO-SrO multilayers. The $(BiO)_2$ planes contribute as a charge reservoir. The CuO_2 planes function as the conduction planes of superconductive current. From the crystallographic point, the three-layered Bi-2223 compound has to demonstrate highly anisotropic (quasi two-dimensional) physical properties, and again this study strongly requires the availability of high quality and large size single crystals.
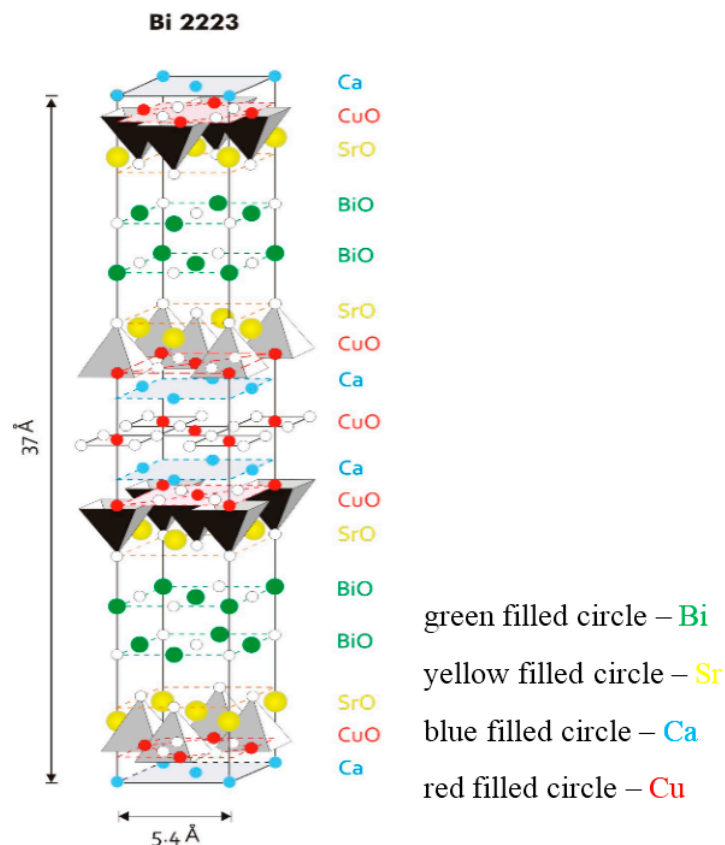

Figure 1. Crystal structure of Bi-2223 phase.

2. Main Growth Difficulties

Whereas the Bi-2201 and Bi-2212 compounds could be directly synthesized either from a melt or using a standard solid state reaction [2,3,6,7], the Bi-2223 phase is quite difficult to prepare with acceptable purity even in powder form [8]. The question of phase formation is highly debated in literature, and different mechanisms have been proposed [8–10]:

(i)   a direct phase transformation from Bi-2212 into Bi-2223 through the insertion of additional Ca and Cu–O layers into the structure;

(ii) a disproportionation reaction 2· Bi-2212 → Bi-2223 +Bi-2201; and

(iii) a nucleation and growth from a liquid phase.

Therefore, even the selection of a nominal composition for a Bi-2223 solid state synthesis is not obvious. In addition, the thermal stability range of Bi-2223 material is much smaller compared with Bi-2201 and Bi-2212 phases. According to [1], the Bi-2223 compound is stable only in a very narrow temperature range of about 50 °C just below the incongruent melting line. For comparison, Bi-2212 compound is stable in a wide temperature range between 650 °C and 895 °C [1]. Thus, the Bi-2223 phase solid state synthesis with acceptable purity has been a particularly difficult task. Moreover, the sluggish formation rate known for Bi-2223 phase makes this task even more arduous [11]. The $Bi_2O_3(PbO)$-SrO-CaO-CuO system contains four or even five components that strongly complicates the phase equilibria investigations especially taken into account that this system has a certain tendency for a glassy behavior.

It was reported that the partial substitution of Bi by Pb can effectively enhance the phase formation kinetics as well as increase the yield of Bi-2223 phase [12]. The formation of Bi(Pb)-2223 phase is highly accelerated by the partial melting of Pb-doped samples. Nevertheless, the Pb-doped Bi-2223 samples are less attractive objects for the fundamental research because the substitution of Bi by Pb gives rise to additional complications in interpretation of physical measurements. From this point, high-quality Pb-free Bi-2223 crystals are in great demand for the fundamental research.

A very interesting *in-situ* investigation of growth mechanism for compositions near the $Bi_2Sr_2Ca_2Cu_3O_y$ stoichiometry has been done in [13]. The authors used high-temperature optical microscope for *in-situ* observation of melting and solidification processes. The solidified bodies were studied by EDX/SEM analysis. The authors made a conclusion that no nucleation and no growth of Bi-2223 were observed directly from a melt in all experiments independent from a starting composition. The Bi-2223 crystals were formed peritectically at 870 °C for 6.5%O_2/93.5%Ar atmosphere according to reaction: $(Sr,Ca)CuO_x$ + Bi-rich melt → Bi-2223. In air Bi-2223 phase was formed according to another peritectic reaction: $(Sr,Ca)_{14}Cu_{24}O_x$ + Bi-rich melt → Bi-2223. In both cases, long-lasting annealing of about 50 h was required to observe the formation of Bi-2223 compound when $Bi_{2.5}Sr_2Ca_{1.3}Cu_{3.2}O_y$ starting composition has been used. No Bi-2223 crystals were found when stoichiometric Bi-2223 composition was utilized. These results are fully inconsistent with data given in [8,14] where Bi-2223 material could be formed throughout the normal nucleation and growth within the primary crystallization field. The observed in [13] Bi-2223 peritectic growth and the absence of a primary crystallization field could explain well why extremely low growth rates of 0.04–0.05 mm/h are necessary for the floating zone (FZ) growth of Bi-2223 crystals [15] compared with other Bi-based superconductors. It seems that the question of phase formation and thermal stability of Bi-2223 compound is still unclear and requires further investigations. All together, it makes well understandable why the growth of Bi-2223 crystals has been a main challenge for crystal growers since the discovery of this compound in 1988 although a numerous efforts were done including flux and FZ growth.

Another commonly observed problem is Bi-2212 (Bi-2201) intergrowth lamellae in Bi-2223 matrix [11,15]. Most intergrowth lamellae have the thickness of unit cell or half-unit cell. Figure 2 shows the typical HRTEM image of Bi-2223 single crystal grown by FZ method with electron beam parallel to the *b*-axis [11].
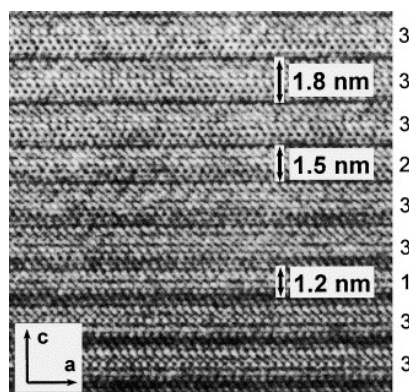
Figure 2. HRTEM image [11] of Bi-2223 crystal, showing the coexistence of Bi-2223, Bi-2212 and Bi-2201 phases. Reprinted with permission from Elsevier. All rights reserved.

Lamellae of different phases can be observed. Main lamellae with a spacing of ~18 Å corresponded to the Bi-2223 phase (denoted as "3" in the Figure 2). Some shorter lamellae with spacing of ~15 Å and ~12 Å (indicated by "2" and "1" in the Figure 2, respectively) are the intergrowth of Bi-2212 and Bi-2201 phases. The intergrowth is a typical stacking fault of layers within a crystal with an extension of one-half to several unit cells in the direction of the crystallographic *c*-axis [15]. According to numerous observations, there is no regularity in the sequence of intergrowth phases. In low-quality Bi-2223 crystals, the amount of Bi-2212 phase might be up to 20 wt.% due to the intergrowth problem, while the good quality crystals contain 2–3 wt.% of Bi-2212 phase only. Although the HRTEM is a nice tool to observe the intergrowth, the preparation of samples by ion-beam milling after cut perpendicular to Bi-2223 layers is special, sophisticated and time-consuming procedure. In addition, the HRTEM is a local probe. Another method to identify a possible Bi-2212 intergrowth in Bi-2223 sample is magnetic measurements of SC transition in a zero-field cooled (ZFC) regime. Researchers observed a small (usually <2%) step-like decrease in the magnetization at around 80 K [11,15] on the good quality samples caused by Bi-2212 intergrowth. It was shown in [16] that X-ray diffraction (XRD) technique is a more sensitive tool to probe the intergrowth than ZFC magnetic measurements. Effects of oscillated broadening and peak shift of the (0 0 L) Bragg reflections were revealed in Bi-2223 crystals [16]. This diffraction phenomenon is well known for a random intergrowth of a secondary phase (here it is Bi-2212). The oscillation amplitude is proportional to the defects concentration if it is relatively low. It enables the authors [16] to estimate the content of intergrowth defects to be about 2 wt. % even for the "intergrowth-free" samples according to ZFC measurements. This approach was found to be rather universal being applicable for other layered Bi-based superconductors [17]. Thus, not only the growth of Bi-2223 crystals is a hard task but the correct characterization of as-grown samples requires special attention, too.

3. Growth History

The self-flux method is often used to grow high-Tc superconductors because of its simplicity. However, in systems with a narrow primary crystallization field, the flux method allows a preparation of tiny crystals embedded in a solidified melt only. Since Bi-2223 has a very narrow crystallization field [1,14], growth by self-flux was thought to be almost impossible. There were a few attempts to prepare Pb-free and Pb-doped Bi-2223 single crystals using molten KCl salt [18,19]. Only very small samples with dimensions up to 100×100 μm^2 in (*a*,*b*) plane and thickness of 1–5 μm along *c*-axis were obtained. In general, Bi-2223 crystals contained 2–3 wt.% of Bi-2212 phase due to the intergrowth problem. The presence of Bi-2212 intergrowth was detected by both XRD and ZFC magnetic measurements [19]. In addition, the presence of $(Ca,Sr)CuO_2$ and CuO impurity phases was often observed in XRD patterns. The most detailed investigation of this synthetic route is given in [20].

The authors used pre-sintered at 880 °C precursors getting the cation compositions Bi:Sr:Ca:Cu = 2:2:2:3 and 2:2:2:4. The obtained oxide powders (solute) were mixed with KCl (solvent) in ratio 1:4 and 1:10 and used as a charge for the crystal growth. The synthesis was performed in Al_2O_3, MgO and Pt containers. The crystals were grown by isothermal heat treatment of charge material at 800–880 °C for 15 and 100 h. In some cases, a low cooling rate of 0.5–1.0 °C/h was applied to reduce the effect of KCl evaporation. It was found that the best samples were obtained in high-density MgO crucibles. It was shown that the interaction of MgO with the KCl melt and components of oxide precursor, as well as Bi-2223 contamination by Mg is negligible. The optimal temperature range for the Bi-2223 phase formation and crystal growth was found to be very narrow (860–870 °C) and located just below the peritectic melting of oxide precursor in the KCl melt. At the first stage of isothermal heat treatment (<15 h), rapid formation of almost pure Bi-2223 phase was demonstrated by X-ray diffraction. The same process without KCl leads to the formation of samples dominated by the Bi-2212 phase. The rapid formation of Bi-2223 material in presence of molten KCl was explained based on the "dissolution-precipitation" mechanism and high activity of Cu ions in the KCl melt [20]. Since the transformation of Bi-2212 into Bi-2223 phase needs a long-lasting annealing, the fast KCl evaporation is not favorable for the Bi-2223 crystal growth. In order to reduce the flux evaporation, a very effective tool was the crucible covering with a lid and increasing of solute/solvent ratio. It was shown that individual crystals with dimensions of about 100×100 μm^2 and thickness up to 5 μm have been prepared after isothermal treatment for 15 h, while the samples larger than 500×500 μm^2 in (*a,b*) plane were obtained after 100 h treatment. After growth, the solidified KCl melt was washed out using distilled water and further rinsing in acetone. For the as-grown samples, a superconducting transition at T_c *(onset)* = 109 K was detected by magnetization and resistivity measurements.

A very interesting growth approach has been developed in [21,22]. The authors have used the laser-assisted floating zone technique to prepare superconducting fibers with diameter approximately 1 mm and length up to 20 mm. The as-grown fibers were not single-phase and contained tiny Bi-2212 and Bi-2223 crystallites elongated along growth direction. The fibers demonstrated maximum T_c up to 110 K after post-growth annealing from resistivity measurements.

Usually, the flux method is not suitable for the growth of materials with a narrow primary crystallization field when the control of crystals nucleation and growth is rather hard. In addition, it is important to keep the solvent composition and quantity at the specific optimal values for the flux steady growth. The last one requires the detailed knowledge of a corresponding phase diagram. Unfortunately, it is not a case for nearly all four-component systems including Bi_2O_3-SrO-CaO-CuO one. Thus, all flux-grown Bi-2223 crystals were very thin with dimensions up to $1.0 \times 0.5 \times 0.005$ mm^3. From this point, the crucible-free FZ method is much more suitable for the growth of larger crystals, because, in general, the crystal growth is performed continuously at one point on the temperature-composition phase diagram. In this case there is no need in detailed knowledge of primary crystallization field. Moreover, in FZ growth of Bi-based superconductors, the molten zone (MZ) composition is self-adjusted during the growth if molten zone is well stable against the compositional and temperature fluctuations [11,15]. The stability of MZ depends on many factors: quality of feed rod, pulling rate, temperature gradient in a hot zone, applied gas pressure and so on. Usually, it is expected that the MZ can be kept more stable if its length is reduced, because the MZ is supported only by surface tension against gravity. For the image furnaces equipped with halogen lamps the length of MZ mainly depends from the thickness of lamp filament. Thus, the higher is a nominal lamp power, the larger is the zone length. In addition, it was found in [15] that a steep temperature gradient in a hot zone plays a very important role in maintaining a stable MZ for Bi-2223 growth. Another crucial condition for the growth of large size single crystals is a planar growth front. Both slow pulling rates and large temperature gradients are expected to prevent a constitutional supercooling, which is the origin of the opposite cellular crystallization front. In general, an image furnace equipped with halogen lamps provides much higher (10–100 times) temperature gradients on crystallization front compared with other crucible-based techniques like Flux, Bridgman and Top Seeded Solution Growth methods. The

steep temperature gradient stabilizes a planar crystallization front at low pulling rates that leads to the growth of larger crystals. Moreover, this growth approach is a crucible free and, thus, has no crucible contamination problem. All together it makes FZ method to be quite promising for the Bi-2223 crystal growth

In addition, it is quite interesting to compare the technical specifications of image furnaces produced by different companies. The NEC (Japan) image oven is equipped with 500 W and 1500 W halogen lamps, and the lower limit of pulling rate is 0.5 mm/h for a standard setup. The CSI (Japan) image furnaces got halogen lamps with nominal lamp power ranging from 150 W to 1500 W. In addition, the lowest pulling rate is about 0.04–0.05 mm/h. The comparison obviously demonstrates that a CSI image furnace provides much better growth conditions than a NEC one. Moreover, the four-mirrors CSI optical setup gives much less pronounced thermal fluctuations in a horizontal plane compared with double-mirrors NEC optics. The SciDre GmbH (Germany) produced an image oven that allows one to reach extremely high gas pressures up to 150 bars. The last value is the world record for all image furnaces. For example, the CSI and NEC machines have the upper gas pressure limit of 10 bars. The lowest pulling rate for SciDre oven is 0.1 mm/h that makes it suitable for the growth of Bi-2201 and Bi-2212 superconductors. On the other hand, the SciDre furnace is equipped with an arc lamp. In general an arc lamp provides less stable molten zone at low pulling rates ($\leqslant$1.0 mm/h) compared with a halogen lamp due to the tiny position fluctuations of the arc hottest point. This is the main reason why image furnaces equipped with arc lamps have been never used successfully for the growth of high-T_c cuprates. To the author's experience, the CSI image furnace is the best tool for the growth of all Bi-based superconductors.

The first successful Bi-2223 FZ growth has been performed in 2001 [15]. The main clue of this success was: (i) applying an extremely low growth rate of 0.04–0.5 mm/h; and (ii) using 300 W halogen lamps. The authors found that the temperature gradient was 350 °C/cm in the hot zone for 300 W lamps, which was two times larger than that with 1500 W lamps. In addition, the length of MZ was reduced from 4.0 to 4.5 mm (1500 W lamps) to 3.5–4.0 mm (300 W lamps), which made MZ quite stable over the whole growth time (3–4 weeks). The most detailed investigations of the Bi-2223 crystal growth by FZ method has been done in [11,16,23,24] and is discussed in the next section.

4. FZ Growth of Pure and Pb-Doped Samples

According to [11,16,23], $Bi_{2.1}Sr_{1.9}Ca_{2.0}Cu_{3.0}O_y$ is the best feed rod composition for FZ run being slightly Bi-rich similar to the Bi-2212 growth. The feed rods for the crystal growth were prepared by the conventional solid state method. Powders of Bi_2O_3, $SrCO_3$, $CaCO_3$ and CuO (all of 99.9% purity) with cation ratio Bi:Sr:Ca:Cu = 2.1:1.9:2.0:3.0 were well mixed and calcined at 780 °C for 48 hours in air with intermediate grindings. The calcined powder was formed into cylindrical rods ($\sim\phi$ 6 × 80 mm). The rods were hydrostatically pressed under a pressure of ~70 MPa and sintered at 850 °C for 50 h in air. Prior to the crystal growth, the high-density feed rod (~90% of the crystal density) was obtained by pre-melting the as-sintered rod at a rapid rate of 25 mm/h. The quality of the pre-melted feed rods is critical for the FZ technique because during the crystal growth the molten zone is sustained by the feed rod through a surface tension. A straight, dense and equal-diameter feed rod is required to stabilize the molten zone over a long growth period. Schematic illustration of the FZ growth setup and snapshot of the real growth process are shown in Figure 3.

The feed rod is hung up on the upper shaft using Ni wire and seed is fixed rigidly to the lower shaft. Both feed and seed rods are placed coaxially in the center of a quartz tube. The halogen lamps are used as the radiation source, and ellipsoidal mirrors utilized to focus the light in the vicinity of the contact between feed and seed rods. A molten zone is formed between upper and lower rods by melting the feed rod tip. The mirror's stage is moved upward, and the molten zone passes through the feed rod. In turn, the growing crystal is solidified on the crystallization border.

Single crystals were grown using the CSI image furnace equipped with four halogen lamps. A sharp temperature gradient of ~300 °C/cm along the molten zone was obtained using 300 W lamps.

A short pre-melted feed rod (~20 mm in length) was used as a seed rod in the crystal growth. Both the feed and seed rods were counter rotated (25 rpm and 15 rpm) to minimize the diffusion layer close to the crystallization front. The mixed gas flow of argon and oxygen was applied. Due to the highly anisotropic crystallization rates for Bi-based superconductors, it is very difficult to obtain thick single crystals along the *c*-axis. Therefore, slow growth rates of 0.20, 0.10, 0.06 and 0.04 mm/h were used in an attempt to obtain large crystals. The experimental conditions are summarized in Table 1.
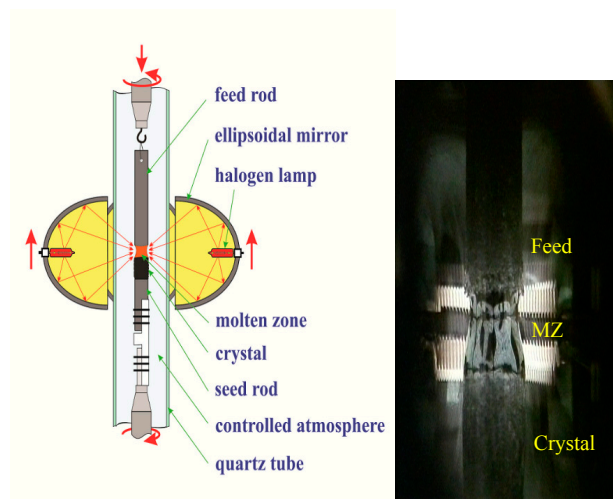
Figure 3. FZ growth setup (**left**); and snapshot (**right**) of the real Bi-2223 growth process.

Table 1. Growth conditions, crystal compositions from EDX analysis, presence of dominant phase determined from XRD and ZFC measurements, and T_c of Bi-2223 single crystals.

Feed Rod Composition	Crystal Composition	Growth Atmosphere	Growth Rate (mm/h)	Dominant Phase	$T_{c, onset}$ (K)
$Bi_{2.1}Sr_{1.9}Ca_2Cu_3O_{10+\delta}$	$Bi_{2.18}Sr_{1.82}Ca_{1.27}Cu_{2.15}O_{10+\delta}$	80% Ar + 20% O_2	0.20	Bi-2212	80
$Bi_{2.1}Sr_{1.9}Ca_2Cu_3O_{10+\delta}$	$Bi_{2.16}Sr_{1.84}Ca_{1.32}Cu_{2.34}O_{10+\delta}$	80% Ar + 20% O_2	0.10	Bi-2212	93
$Bi_{2.1}Sr_{1.9}Ca_2Cu_3O_{10+\delta}$	$Bi_{2.08}Sr_{1.92}Ca_{1.69}Cu_{2.69}O_{10+\delta}$	80% Ar + 20% O_2	0.06	Bi-2223	102
$Bi_{2.1}Sr_{1.9}Ca_2Cu_3O_{10+\delta}$	$Bi_{2.11}Sr_{1.89}Ca_{1.83}Cu_{2.87}O_{10+\delta}$	20% Ar + 80% O_2	0.04	Bi-2223	103

Figure 4 shows plate-like Bi-2223 single crystals cleaved from as-grown ingot prepared at 0.05 mm/h growth rate. Laue X-ray back-reflection photography revealed that these plates are the (001) crystallographic plane. All crystals are elongated along *a*-axis (*i.e.*, the growth direction is [100]).
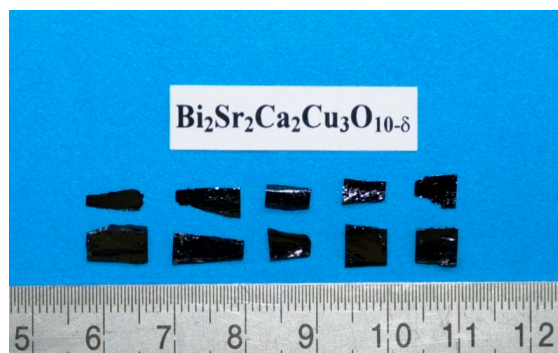

Figure 4. Cleaved Bi-2223 single crystals. The small grid division is 1 mm.

The composition of each ingot was determined by EDX analysis. The results are summarized in Table 1. The compositions of crystals grown at slow rates of 0.04–0.06 mm/h are close to Bi-2223 phase. However, the compositions of crystals obtained at rates of 0.10–0.20 mm/h are closer to Bi-2212 phase, indicating that the faster growth rates are unfavorable for the formation of Bi-2223 phase. In order to examine the homogeneity of composition throughout as-grown ingots, crystals were selected at intervals of 1 cm along the ingots and measured by EDX analysis. The atomic compositions of each crystal were derived by averaging data measured on three or four points of each crystal. Figure 5 shows the atomic percentages of Bi, Sr, Ca, and Cu at different positions of the ingot obtained with growth rate of 0.06 mm/h under mixed gas flow of 80% Ar and 20% O_2. It can be seen that the fluctuation of the composition is quite low except for the initial part of the ingot. This implies that the molten zone was quite stable during the growth except for the beginning. Indeed, it was observed during the growth that the stability of the molten zone of Bi-2223 is higher than those of the Bi-2201 and Bi-2212, which reflects that the self-adjustability of the Bi-2223 melt composition is rather high.
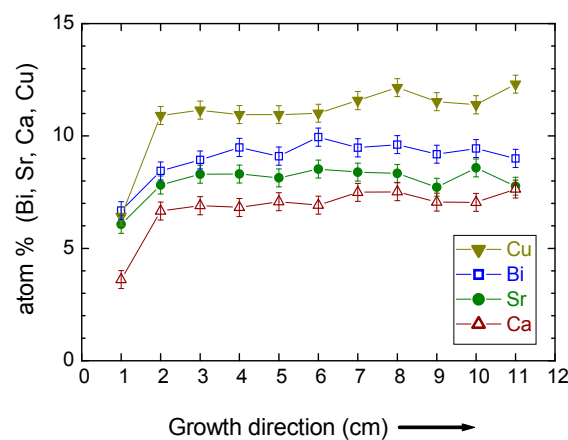

Figure 5. Atomic composition from the EDX analysis *versus* the growth length [11]. Reprinted with permission from Elsevier. All rights reserved.

The composition of MZ during the Bi-2223 growth was studied in [16]. Two specimens were frozen by quenching the molten zones after running three and 20 days, respectively. The composition of each frozen zone was measured by ICP-AES analysis. The results of the chemical analysis are listed in Table 2. The data indicate that the molten zone composition comes into equilibrium after a three-day run already, remaining practically invariable thereafter.

Table 2. MZ composition after three- and 20-days of FZ growth compared with feed rod composition.

Composition	3-Day's Specimen	20-Day's Specimen	$Bi_{2.1}Sr_{1.9}Ca_{2.0}Cu_{3.0}O_y$
Bi (at.%)	32.6 ± 0.5	32.0 ± 0.6	23.3
Sr (at.%)	19.9 ± 0.4	20.8 ± 0.4	21.1
Ca (At.%)	13.3 ± 0.4	13.5 ± 0.5	22.2
Cu (at.%)	34.2 ± 0.4	33.7 ± 0.5	33.4

When compared with the initial feed rod composition, one can easily see that the liquid zone content of Sr and Cu remains invariant, whereas the content of Ca in the molten zone is definitely lower compensated by an increased concentration of Bi. As a result, the composition of the liquid being in the equilibrium with the Bi-2223 phase is Ca-depleted and Bi-rich for FZ run. The similar effect was observed for the laser-assisted FZ growth of Bi-2212 superconducting fibers [25,26]. The authors [25,26] explained this effect in terms of effective distribution coefficients that being less (for Bi) and greater (for Ca) than unit. In addition, the results of [16] showed that the Bi-2223 crystal growth at 0.06 mm/h is quite sensitive to the oxygen content in gas environment, and the low-oxygen limit is about 2.5%.

According to the magnetic measurements the majority of crystals grown at 2.5% oxygen content are Bi-2212 while the same growth procedure at 5%, 10% and 20% oxygen contents leads to the Bi-2223 growth. In addition, the ingot prepared at 2.5% oxygen content contained a visible amount of Ca_2CuO_3 impurity phase.

For growing the Pb-doped crystals, the commonly used image furnace setup was modified by adding an internal source of Pb [27]. According to [28,29] a Pb loss at high temperatures has to be minimized in order to keep the stoichiometry of the sample close to the nominal one, thus promoting equilibrium phase formation. This can be done either by applying a high pressure [28] to prevent Pb evaporation or by enclosing samples in sealed tubes [29] to saturate the atmosphere with Pb vapor. Unfortunately, neither of these methods can be utilized in FZ growth. For these reasons, the authors in [27] developed a new technique called as VA-FZ (Vapor Assisted Floating Zone) by adding an internal source of Pb vapor. An Al_2O ring crucible containing PbO encircling the seed rod was placed inside the quartz tube close to the molten zone. The position of the PbO source was accurately chosen so that the temperature of the ring crucible was around 750 °C, and the PbO evaporation rate was about 2×10^{-8} mole/h, determined by preliminary TG experiments. This allowed the authors [27] to compensate the Pb loss from the MZ by means of a lead evaporation from the PbO source.

The feed rod composition was Bi:Pb:Sr:Ca:Cu = 1.84:0.32:1.84:1.97:3.00. The crystal growth was performed at low travelling rates ranging from 0.03 to 0.20 mm/h, and the best samples have been grown at 0.05-0.06 mm/h. Both pre-melting and crystal growth were carried out under flowing 93% Ar–7% O_2 gas mixture. Pre-melting of as-sintered feed rod was done at 25 mm/h. Large (Bi,Pb)-2223 crystals with typical dimensions up to *2.0 × 3.0 × 0.1* mm^3 have been prepared by VA-FZ method. The Pb content in as-grown samples was found to be Bi:Pb:Sr:Ca:Cu = 2.16:0.26:2.08:1.95:2.65. This indicates that this growth technique was successful in compensation of Pb evaporation from the molten zone during the long-lasting growth run. The superconducting transition was observed at T_c = 106 K, and the width of transition, ΔT_c = 3 K, was smaller compared with Pb-free Bi-2223 crystals. The Pb-doped crystals have orthorhombic structure, but the orthorhombic distortion is enhanced and the *c*-axis cell parameter is found to be slightly larger compared with Pb-free Bi-2223 samples. The lattice parameters are the following: *a* = 5.395(1) Å, *b* = 5.413(1) Å and *c* = 37.04(1) Å. The structure of lead-doped samples was modulated with a modulation vector *q* ~ 0.21*a*, as confirmed by the presence of satellites in the diffraction pattern. The high quality of as-grown crystals allowed the observation of satellites of up to the third order.

5. Crystal Characterization

Single-crystal XRD measurements were made on a number of Pb-free as-grown Bi-2223 crystals [23] chosen from each ingot to check the crystallinity of as-grown samples. Figure 6 shows a typical single-crystal XRD patterns for the crystal grown at a rate of 0.04 mm/h. Only sharp (00*l*) peaks are observed, indicating the good crystallinity of the sample. All diffraction peaks can be indexed into the Bi-2223 phase with the *c*-axis lattice parameter of 36.552(6) Å.
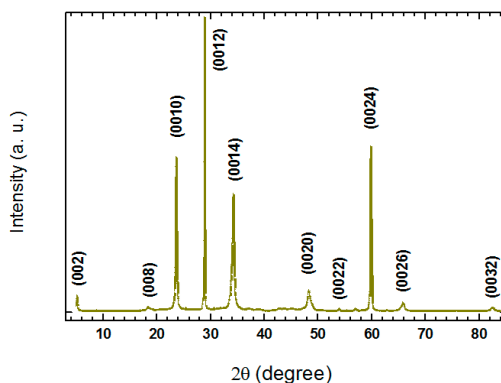

Figure 6. Single-crystal XRD pattern of as-grown Bi-2223 crystal prepared at 0.04 mm/h rate [23].

Powder XRD measurements were performed on ground crystals in order to examine the presence of impurity phases as well as to determine the crystal structure and lattice parameters. Figure 7a–c present the powder XRD patterns for three as-grown crystals obtained using growth rates of 0.20, 0.10 and 0.04 mm/h, respectively. It is noteworthy that the growth rate dramatically influences the phase formation of crystals. The crystals obtained at a rate of 0.20 mm/h exhibit majority phase of Bi-2212 and small amount of Ca_2CuO_3 and some unidentified phases, as shown in Figure 7a. No Bi-2223 phase could be detected from these crystals. The crystals grown at a slower rate of 0.10 mm/h consist of Bi-2212, Ca_2CuO_3 as well as a small amount of Bi-2223 phase, as shown in Figure 7b. When growth was performed at a very slow rate of 0.04 mm/h, nearly single-phase crystals, which have >90% Bi-2223 phase, were cleaved from the as-grown ingot, as shown in Figure 7c.
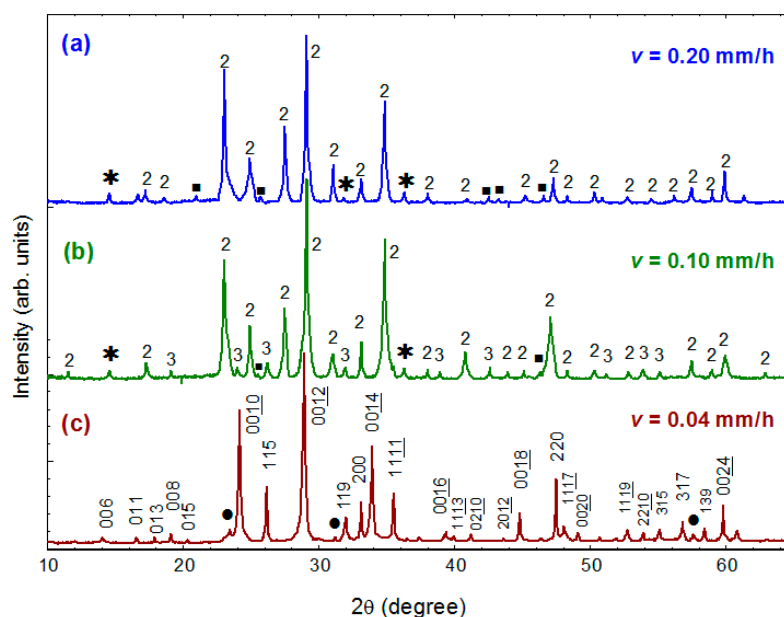

Figure 7. Powder XRD patterns of crystals grown at different rates, revealing the effect of growth rate on the phase formation in crystals: (**a**) 0.20 mm/h, majority phase Bi-2212; (**b**) 0.10 mm/h, Bi-2223 phase appeared; and (**c**) 0.04 mm/h, nearly pure Bi-2223 phase. "3", "2", "*" and "■" indicate Bi-2223, Bi-2212, Ca_2CuO_3 and unidentified phases, respectively. The diffraction peaks of Bi-2223 phase in Figure 7c are indexed with respect to the space group *A2aa*. A few weak peaks corresponding to the Bi-2212 phase are marked with "●" in this pattern [11]. Reprinted with permission from Elsevier. All rights reserved.

Using a least-square refinement program, the nearly single-phase Bi-2223 crystals were determined to be of orthorhombic structure with the lattice parameters *a* = 5.408(2) Å, *b* = 5.413(7) Å and *c* = 36.868(1) Å (space group *A2aa*). These results demonstrate that a faster growth rate is unfavorable for the formation of Bi-2223 phase due to the extremely narrow crystallization field and complex melting behavior.

A large number of as-grown crystals from each ingot were checked using magnetic susceptibility measurements. Sintered and pre-melted feed rods were also measured for comparison. The results of magnetic measurements reveal that the crystal growth rate apparently influences the phase formation in crystals. Figure 8 shows the temperature dependence of the real part of AC susceptibility measured on sintered and pre-melted feed rod as well as on as-grown crystals obtained at different growth rates. Both sintered and pre-melted feed rods exhibit very broad superconducting transitions with onset $T_c \sim 80$ K, indicating that the principal superconducting phase in feed rods is Bi-2212 phase with an inhomogeneous oxygen distribution.
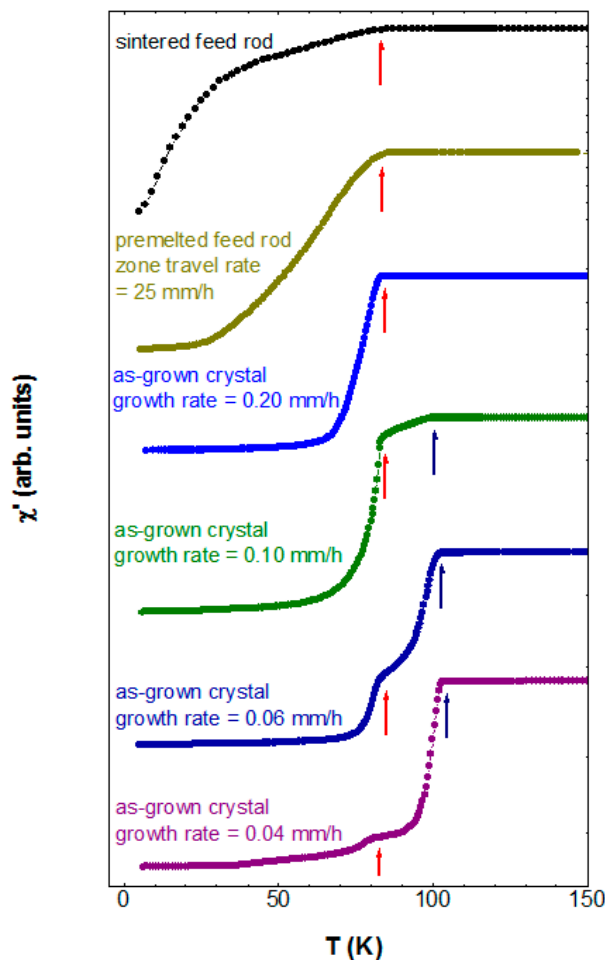
Figure 8. Temperature dependence of AC susceptibility measured on sintered feed rod, pre-melted feed rod and crystals grown with different rates, showing the effect of growth rate on the phase formation of Bi-2223 crystals. Only the real part (χ') of AC susceptibility is plotted [11]. Reprinted with permission from Elsevier. All rights reserved.

The crystal grown at a rate of 0.20 mm/h exhibits a relatively sharp transition also around 80 K. No trace of a transition around 110 K could be seen, implying that the majority superconducting phase in fast-grown crystals is still Bi-2212 with relatively homogeneous oxygen distribution. When the growth rate decreases to 0.10 mm/h, the as-grown crystal displays two superconducting transitions around 100 and 80 K, corresponding to Bi-2223 and Bi-2212 phases, respectively. When the growth rate slows down further to 0.06 mm/h, the Bi-2223 phase is determined to be dominant in crystals. When an extremely slow growth rate of 0.04 mm/h was used, the as-grown crystals have >90% of Bi-2223 phase.

Finally, the more complicated crystallization behavior of Bi-2223 phase and its lower thermal stability compared with other Bi-based superconductors required for the FZ growth of nearly pure Bi-2223 samples almost one order less pulling rates (0.04–0.06 mm/h) compared with the growth of Bi-2201 (0.5–1.0 mm/h) and Bi-2212 (0.2–0.5 mm/h) materials.

6. Effect of Post-Growth Treatment on Superconductivity

Post-annealing experiments were carried out at 500–850 °C for 120–500 h to improve the crystal quality with respect to phase purity and oxygen homogeneity [30]. The annealing conditions are listed in Table 3. The effect of oxygen annealing was studied by both XRD and magnetic susceptibility measurements. A phase-transform process from Bi-2212 to Bi-2223 was observed.

Table 3. Annealing conditions and results for Bi-2223 single crystals.

Temperature (°C)	Time (h)	Atmosphere	Phases	$T_{c, onset}$ (K)
500	120	O_2 flow	Bi-2223, Bi-2212, Ca_2CuO_3	105
600	120	air	Bi-2223, Bi-2212, Ca_2CuO_3	105
650	120	O_2 flow	Bi-2223, Bi-2212, Ca_2CuO_3	106
750	120	O_2 flow	Bi-2223, minor Bi-2212	106
850	360	O_2 flow	Bi-2223	108
850	500	O_2 flow	Bi-2223	110

Such a phase transformation might be explained via a layer-intercalation mechanism, which suggests that Bi-2212 phase can be transformed to Bi-2223 phase through layer-by-layer intercalation of the Ca-Cu-O bi-layers into the existing Bi-2212 structure [31]. Figure 9 shows the temperature dependence of AC susceptibility measured on Bi-2223 as-grown and annealed crystals. The as-grown crystal shows two superconducting transitions around 102 and 80 K, corresponding to Bi-2223 and Bi-2212 phases, respectively. As the annealing temperature is elevated and/or the annealing time increased, the transition at 80 K is gradually suppressed, indicating a decrease of the Bi-2212 phase. The crystal annealed at 850 °C for 500 h shows a sharp transition at 110 K with only a small remnant at 80 K. This indicates that nearly single-phase Bi-2223 crystals were obtained using slow growth rates (⩽0.06 mm/h) and subsequent long-time annealing. The result of susceptibility measurements does not only demonstrate the influence of annealing on the phase transformation in crystals but also shows the effect of annealing on the superconductivity of Bi-2223 crystals. As shown in the inset of Figure 9, the onset T_c increases from 102 K for the as-grown crystal to 110 K for the crystal annealed at 850 °C for 500 h.
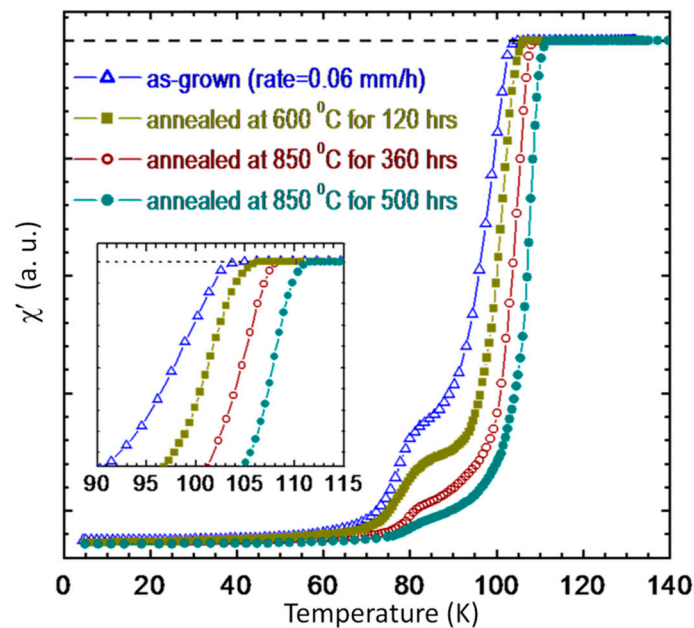

Figure 9. Temperature dependence of AC susceptibility measured on as-grown crystal prepared at 0.06 mm/h (Δ) and crystals annealed: at 600 °C for 120 h (■), 850 °C for 360 h (○) and 850 °C for 500 h (●). Only the real part (χ') of AC susceptibility is plotted. The curves have been mass normalized to unity for the sake of comparison [11]. Reprinted with permission from Elsevier. All rights reserved.

Usually, it is difficult to precisely determine the oxygen content for single crystals, particularly for the large ones; however, from the tendency of T_c's change observed from our annealing experiments, one can suggest that the as-grown Bi-2223 crystals are in the slightly under-doped region. It is

interesting that further increasing of oxygen pressure up to 500 bars during the annealing remains the T_c to be unchangeable around 110 K [30].

In order to demonstrate more clearly the phase evolution with annealing temperature and/or time, powder XRD measurements were performed on a ground crystal before and after oxygen annealing. The results are presented on Figure 10a–d. Prior to annealing, Bi-2223 was the dominant phase in the as-grown sample. However, the Bi-2212 and Ca_2CuO_3 phases were also observed, as shown in Figure 10a. After being annealed in O_2 flow at 600 °C for 120 h, the intensity of the Bi-2212 and Ca_2CuO_3 peaks decreased, as shown in Figure 10b. Using the high temperature annealing at 850 °C for 500 h a nearly single-phase Bi-2223 crystal was obtained (Figure 10d). All diffraction peaks in Figure 10d can be assigned to the Bi-2223 phase with orthorhombic symmetry. These results confirmed a nearly complete conversion of Bi-2212 phase into Bi-2223 one (Bi-2223 content >98%).
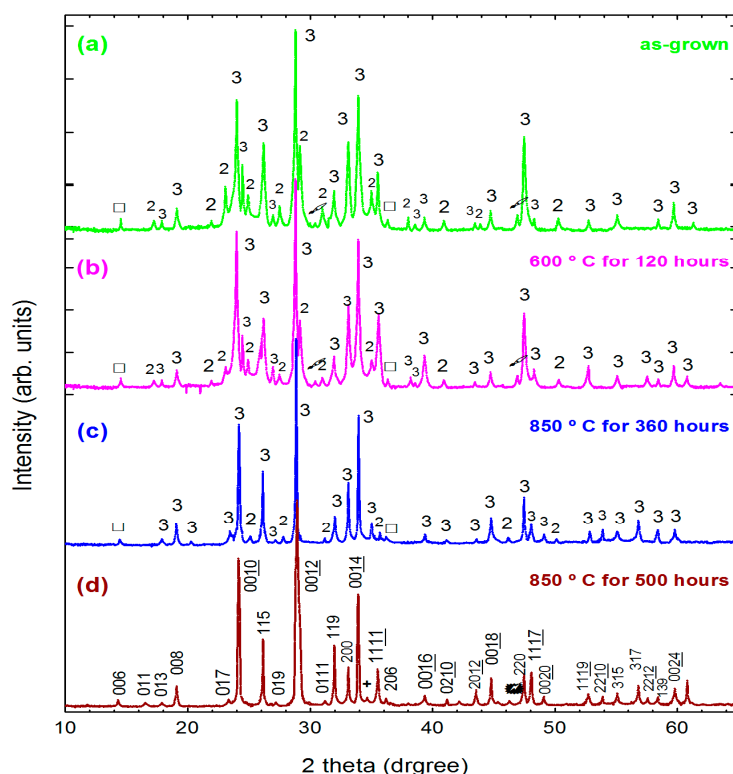

Figure 10. Powder XRD patterns of as-grown and annealed in oxygen flow Bi-2223 crystals: (**a**) as-grown sample; (**b**) 600 °C for 120 h; (**c**) 850 °C for 360 h; and (**d**) 850 °C for 500 h. "3", "2" and "□" indicate Bi-2223, Bi-2212 and Ca_2CuO_3 phases, respectively. The Bi-2223 diffraction peaks in (d) are indexed in the space group A2aa. A few weak Bi-2212 peaks are shown with "+" [30]. © IOP Publishing. Reproduced with permission. All rights reserved.

This transformation from one member of the structural family into another can be understood via a layer-intercalation mechanism [31]. According to this mechanism, the Bi-2212 phase could be transformed into the Bi-2223 compound via intercalating the CuO_2/Ca bi-layers into the CuO_2/Ca/CuO_2 blocks of the existing Bi-2212 structure. This kind of phase conversion is diffusion limited and, consequently, is very sluggish even at high temperatures that can be directly seen from Figure 10c–d.

The in-plane and out-of-plane resistances as a function of temperature were measured on selected annealed crystals composed of almost pure Bi-2223 phase. The measured resistance was transformed to the respective resistivity ρ_{ab} and ρ_c using the crystal dimensions. Figure 11a,b shows the typical in-plane resistivity ρ_{ab} and out-of-plane resistivity ρ_c as a function of temperature, both of which show very sharp transition at 110 K. The typical T-linear behavior for ρ_{ab} and semiconductive upturn for ρ_c

can be seen. The values of the resistivity for Bi-2223 crystals are of the same order of magnitude as those for Bi-2212 crystals.

Thus, a Bi-2223 crystal quality can be improved after long-lasting post-growth annealing either in oxygen flow or under oxygen pressure. On the other hand, the superconducting transition temperature of the Bi-2223 phase is found to be much less sensitive to oxygen doping than Bi-2212, and only small variations of T_c are observed after different oxygen/argon post-growth treatments. For example, argon annealing at 650 °C for 120 h slightly decreases T_c up to 100 K. The dependence of T_c on oxygen content has been reported in [30,32]. For both publications, authors reported a flat T_c against oxygen doping dependence in the over-doped regime and did not measure any decrease of T_c upon annealing under high oxygen pressures (up to 500 bars). The independence of T_c against oxygen content in the over-doped regime has been interpreted as being compatible with different carrier doping levels in the outer and inner CuO_2 layers [30,32], which would be a unique property of $n \geqslant 3$ Bi-cuprates (n = number of CuO_2 planes).
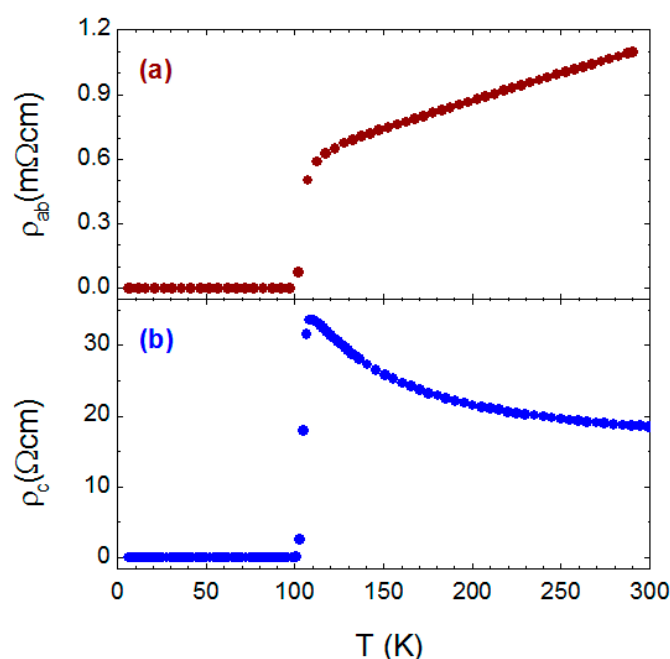

Figure 11. Temperature dependence of (**a**) in-plane and (**b**) out-of-plane resistivity for Bi-2223 crystals annealed at 850 °C for 360 h in oxygen flow [11,30]. Reprinted with permission from Elsevier. All rights reserved.

7. Conclusions

Among all non-toxic high-T_c cuprates, the Bi-2223 material is the most hardly grown one. The reasons for this are threefold: (i) a low thermal stability of lead-free Bi-2223 phase; (ii) a high anisotropy of growth rates caused by layered and complicated crystal structure; and (iii) a tricky melting/solidification behavior. At the same time, the crucible-free floating zone method allows a crystal grower to make nearly single-phase Bi-2223 crystals with dimensions up to $10 \times 6 \times 0.5$ mm^3 suitable for the majority of physical properties measurements. The optimal growth conditions are the following: $Bi_{2.1}Sr_{1.9}Ca_{2.0}Cu_{3.0}O_y$ is the feed rod composition, the pulling rate is 0.04–0.05 mm/h, and the partial oxygen pressure is 0.1–0.2 bar during the growth. Long lasting post-growth heat treatment at elevated temperatures (600–850 °C) in oxygen flow can improve the quality of the as-grown samples. Nevertheless, even the "best" samples contain a few weight percent of Bi-2212 phase due to the intergrowth problem and complications in crystallization process. It is necessary to acknowledge

that a melting behavior and a growth mechanism of Bi-2223 material are still far from our complete understanding, and this calls for further investigations in Bi-2223 crystal growth.

References

1.　Majewski, P. Materials Aspects of the High-temperature Superconductors in the System Bi_2O_3-SrO-CaO-CuO. *J. Mater. Res.* **2000**, *15*, 854–870. [CrossRef]

2.　Liang, B.; Maljuk, A.; Lin, C.T. Growth of large superconducting $Bi_{2+x}Sr_{2-y}CuO_{6+\delta}$ single crystals by travelling solvent floating zone method. *Phys. C* **2001**, *361*, 156–164. [CrossRef]

3.　Gu, G.D.; Takamuku, K.; Koshizuka, N.; Tanaka, S. Large single crystal Bi-2212 along the c-axis prepared by floating zone method. *J. Cryst. Growth* **1993**, *130*, 325–329. [CrossRef]

4.　Jacobs, T.; Katterwe, S.O.; Motzkau, H.; Rydh, A.; Maljuk, A.; Helm, T.; Putzke, C.; Kampert, E.; Kartsovnik, M.V.; Krasnov, V.M. Electron-tunneling measurements of low-T_c single-layer $Bi_{2+x}Sr_{2-y}CuO_{6+\delta}$: Evidence for a scaling disparity between superconducting and pseudogap states. *Phys. Rev. B* **2012**, *86*, 214506. [CrossRef]

5.　Fong, H.F.; Bourges, P.; Sidis, Y.; Regnault, L.P.; Ivanov, A.; Gu, G.D.; Koshizuka, N.; Keimer, B. Neutron scattering from magnetic excitations in $Bi_2Sr_2CaCu_2O_8$. *Nature* **1999**, *398*, 588.

6.　Khasanova, N.R.; Antipov, E.V. Bi-2201 phases synthesis, structures and superconducting properties. *Phys. C* **1995**, *246*, 241–252. [CrossRef]

7.　Takekawa, S.; Nozaki, H.; Umezono, A.; Kosuda, K.; Kobayashi, M. Single crystal growth of the superconductor $Bi_{2.0}(Bi_{0.2}Sr_{1.8}Ca_{1.0})Cu_{2.0}O_8$. *J. Cryst. Growth* **1988**, *92*, 687–690. [CrossRef]

8.　Grivel, J.C.; Flükiger, R. Formation mechanism of the Pb free $Bi_2Sr_2Ca_2Cu_3O_{10}$ phase. *Supercond. Sci. Technol.* **1998**, *11*, 288–298. [CrossRef]

9.　Horiuchi, S.; Shoda, K.; Wu, X.J.; Nozaki, H.; Tsutsumi, M. Phase transition in Bi-based superconductive oxides examined by HRTEM. *Phys. C* **1990**, *168*, 205–214. [CrossRef]

10.　Grivel, J.C.; Flükiger, R. Visualization of the formation of the $(Bi,Pb)_2Sr_2Ca_2Cu_3O_{10+y}$ phase. *Supercond. Sci. Technol.* **1996**, *9*, 555–564. [CrossRef]

11.　Liang, B.; Lin, C.T.; Shang, P.; Yang, G. Single crystals of triple-layered cuprates $Bi_2Sr_2Ca_2Cu_3O_{10+\delta}$: Growth, annealing and characterization. *Phys. C* **2002**, *383*, 75–88. [CrossRef]

12.　Knauf, N.; Harnischmacher, J.; Müller, R.; Borowski, R.; Roden, B.; Wohlleben, D. Preparation and characterisation of single-phase Bi-Pb-Sr-Ca-Cu-O high temperature superconductors. *Phys. C* **1991**, *173*, 414–424. [CrossRef]

13.　Maier, D.; Kulakov, A.B. *In-situ* investigation of phase equilibria and growth mechanisms of compositions near the $Bi_2Sr_2Ca_2Cu_3O_x$ stoichiometry by high-temperature optical microscopy. *Cryst. Growth Des.* **2005**, *5*, 1751–1754. [CrossRef]

14.　Komatsu, H.; Kato, Y.; Miyashita, S.; Inoue, T.; Hayashi, S. *In situ* observations of crystal growth of Bi-based oxide superconductors. *Phys. C* **1991**, *190*, 14–17. [CrossRef]

15.　Fujii, T.; Watanabe, T.; Matsuda, A. Single-crystal growth of $Bi_2Sr_2Ca_2Cu_3O_{10+\delta}$ (Bi-2223) by TSFZ method. *J. Cryst. Growth* **2001**, *223*, 175–180. [CrossRef]

16.　Kulakov, A.B.; Maier, D.; Maljuk, A.; Bdikin, I.K.; Lin, C.T. Study of growth/intergrowth behavior and structural analyses of $Bi_2Sr_2Ca_2Cu_3O_{10+\delta}$ single crystals. *J. Cryst. Growth* **2006**, *296*, 69–74. [CrossRef]

17.　Novomliskii, L.A.; Narymbetov, B.Z.; Zverkov, S.A.; Shekhtman, V.S.; Bush, A.A.; Romanov, B.N.; Ivanov, S.A.; Zhurov, V.V. X-ray diffraction study of highly defected $Bi_4Sr_4CaCu_3O_z$ monocrystals. *Phys. Solid State* **1995**, *37*, 852–860.

18.　Balestrino, G.; Milani, E.; Paoletti, A.; Tebano, A.; Wang, Y.H.; Ruosi, A.; Vaglio, R.; Valentino, M.; Paroli, P. Fast growth of $Bi_2Sr_2Ca_2Cu_3O_{10+x}$ and $Bi_2Sr_2CaCu_2O_{8+x}$ thin crystals at the surface of KCl fluxes. *Appl. Phys. Lett.* **1994**, *64*, 1735–1737. [CrossRef]

19.　Chu, S.; McHenry, M.E. Growth and characterization of $(Bi,Pb)_2Sr_2Ca_2Cu_3O_x$ single crystals. *J. Mater. Res.* **1998**, *13*, 589–595. [CrossRef]

20. Lee, S.; Yamamoto, A.; Tajima, S. Fast synthesis and single crystal growth of Pb-free and Pb-doped Bi-2223 superconductors using alkali chlorides flux technique. *Phys. C* **2001**, *357–360*, 341–344. [CrossRef]

21. Carrillo-Cabrera, W.; Göpel, W.; de la Fuente, G.F.; Verdún, H.R. Preparation and growth of (Bi,Pb)-Sr-Ca-Cu-O superconductor fibers. *Appl. Phys. Lett.* **1989**, *55*, 1032–1034. [CrossRef]

22. De la Fuente, G.F.; Ruiz, M.T.; Sotelo, A.; Larrea, A.; Navarro, R. Microstructure of laser floating zone (LFZ) textured (Bi,Pb)SrCaCuO superconductor composites. *Mater. Sci. Eng. A* **1993**, *173*, 201–204. [CrossRef]

23. Lin, C.T.; Liang, B. Growth of a hard-grown single crystal: $Bi_2Sr_2Ca_2Cu_3O_y$. In *New Trends in Superconductivity*; Annett, J.F., Kruchinin, S., Eds.; Kluwer: London, UK, 2002; Volume 67, p. 19.

24. Giannini, E.; Gladyshevskii, R.; Clayton, N.; Musolino, N.; Garnier, V.; Piriou, A.; Flükiger, R. Growth, structure and physical properties of single crystals of pure and Pb-doped Bi-based high T_c superconductors. *Curr. Appl. Phys.* **2008**, *8*, 115–119. [CrossRef]

25. Costa, F.M.; Silva, R.F.; Vieira, J.M. Diffusion phenomena and crystallization path during the growth of LFZ Bi–Sr–Ca–Cu–O superconducting fibers. *Supercond. Sci. Technol.* **2001**, *14*, 910–920. [CrossRef]

26. Carrasco, M.F.; Silva, R.F.; Vieira, J.M.; Costa, F.M. Pulling rate and current intensity competition in an electrically assisted laser floating zone. *Supercond. Sci. Technol.* **2009**, *22*, 065016. [CrossRef]

27. Giannini, E.; Garnier, V.; Gladyshevskii, R.; Flükiger, R. $Bi_2Sr_2Ca_2Cu_3O_{10}$ and $(Bi,Pb)_2Sr_2Ca_2Cu_3O_{10-\delta}$ single crystals. *Supercond. Sci. Technol.* **2004**, *17*, 220–226. [CrossRef]

28. Lomello-Tafin, M.; Giannini, E.; Walker, E.; Cerutti, P.; Seeber, B.; Flükiger, R. High Pressure Thermodynamic Investigations on the Bi–Pb–Sr–Ca–Cu–O system. *IEEE Trans. Appl. Supercond.* **2001**, *11*, 3438–3441. [CrossRef]

29. Giannini, E.; Savysyuk, I.; Garnier, V.; Passerini, R.; Toulemonde, P.; Flükiger, R. Reversible melting and equilibrium phase formation of $(Bi, Pb)_2Sr_2Ca_2Cu_3O_{10+\delta}$. *Supercond. Sci. Technol.* **2002**, *15*, 1577–1586. [CrossRef]

30. Liang, B.; Bernhard, C.; Wolf, T.; Lin, C.T. Phase evolution, structural and superconducting properties of Pb-free $Bi_2Sr_2Ca_2Cu_3O_{10+\delta}$ single crystals. *Supercond. Sci. Technol.* **2004**, *17*, 731–738. [CrossRef]

31. Cai, Z.X.; Zhu, Y.; Welch, D.O. Layer-rigidity model and the mechanism for ion-diffusion-controlled kinetics in the bismuth cuprate 2212-to-2223 transformation. *Phys. Rev. B* **1995**, *52*, 13035–13040. [CrossRef]

32. Fujii, T.; Terasaki, I.; Watanabe, T.; Matsuda, A. Doping dependence of anisotropic resistivities in the trilayered superconductor $Bi_2Sr_2Ca_2Cu_3O_{10+y}$. *Phys. Rev. B* **2002**, *66*, 024507. [CrossRef]